Quantal Self-Assembly of Polymer Layers in Polypeptide Multilayer Nanofilms

Donald T. Haynie,* Ling Zhang, Wanhua Zhao, and Justin M. Smith

Bionanosystems Engineering Laboratory, Center for Applied Physics Studies, College of Engineering and Science, Louisiana Tech University, PO Box 10348, Ruston, Louisiana 71272

Received April 24, 2006

Simple molecular models predict key aspects of the "microscopic" assembly behavior of various peptide systems in the fabrication of multilayer films. Such films show substantial differences in density for different peptide systems. The data suggest that exponential film growth is possible in the absence of polymer diffusion and that "macroscopic" assembly behavior is more a function of peptide-peptide interactions than peptide sequence alone.

Introduction

It is well established that buildup of a polyelectrolyte multilayer nanofilm by alternate dipping of a charged substrate into solutions of oppositely charged polymers[1−7] is based on the reversal of sign and the "overcompensation" of the net surface charge density.[8] Two general categories of "macroscopic" nanofilm growth mode are described in the multilayer film literature: linear and supralinear.[2,3,5,6] The latter can be called exponential for some polyelectrolyte systems. It is said that the physical basis of exponential growth in a wet film is the inward diffusion of at least one of the two assembling species in a binary polyelectrolyte system.[6] Questions remain, however, concerning mechanisms of nanofilm growth at different levels of structure.

Here, 32mer polypeptides have been designed to probe the physical basis of polyelectrolyte multilayer nanofilm growth with regard to electrostatic interactions, hydrophobic interactions, and hydrogen bonds.[9] The same types of interactions stabilize the folded state of proteins. Data show that model-based predictions of a relative mass increment of 0.5 (1:2), 1 (1:1), or 2 (2:1) in successive polypeptide adsorption steps ("microscopic" level) are corroborated by experiments on four peptide systems. In addition, overall film growth ("macroscopic" level) of a given peptide structure has been found to depend on the electronic character of the peptide assembly partner and therefore on subtleties of interactions between the adsorbing peptides, and film density has been found to have a marked dependence on film architecture.

Experimental Details

The peptide structures were $K_{31}Y$ ("P1"), $E_{31}Y$ ("N1"), $(KV)_{15}KY$ ("P2"), and $(EV)_{15}EY$ ("N2"), where the single-letter code for amino acids is used.[9,10] The backbones of these polymers are identical. Figure 1a shows the chemical structures of E, K, V, and Y, and Figure 1b shows a space-filling model of P2. The side chain of K is basic; E, acidic; V, hydrophobic. The aromatic side chain of Y was for spectroscopic detection. K and E are ionized in solution at neutral pH.[11,12] For P1 and N1, $|\lambda| \approx 1$ in units of electronic charge per amino acid residue at neutral pH; for P2 and N2, $|\lambda| \approx 0.5$. The solubility of P2 and N2 in an aqueous medium is lower than that of P1 and N1 owing to fewer ionized side chains and the relatively large nonpolar surface of the valine side chain.

* Corresponding author. Tel.: +1 (318) 257-3790 (direct). Fax: +1 (318) 257-2562. E-mail: haynie@latech.edu.

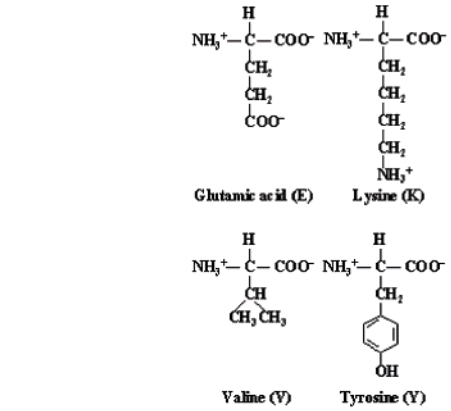

Figure 1. Polymer structure. (a) Chemical structure of amino acid constituents of the peptides studied here. The side chain of E is negatively charged and that of K is positively charged at neutral pH. The side chain of V is hydrophobic. (b) Molecular model of polycation P2 at neutral pH in classical β conformation. The size of the molecule is approximately 10.5 nm × 1.5 nm × 0.5 nm, where the depth measure does not include the natural twist of the molecule. Oxygen atoms, shown in red, define where the plane of the β-pleated sheet, which is perpendicular to the plane of the page, intersects the plane of the page. Carbon is shown in green, nitrogen in blue, hydrogen in white. The lysine side chains point upward, the valine side chains downward. These sets of side chains are on opposite sides of the plane of β-pleated sheet.

Calculated molecular masses of the designed peptides in solution at neutral pH are 4186 Da (P1), 4152 Da (N1), 3735 Da (P2), and 3717 Da (N2), accounting for ionization of side chains and termini. Amino acid composition and purity of the synthetic peptides were assessed by mass spectrometry and high-performance liquid chromatography, respectively. Some sample heterogeneity, due apparently to nonideal monomer coupling, was tolerated; typical nonpeptide polymer preparations in the multilayer film literature are highly polydisperse.

Lyophilized peptides were reconstituted in 10 mM tris(hydroxymethyl)aminomethane, 10 mM NaCl, pH 7.4 at 2 mg/mL. Buffer chemicals, from Sigma-Aldrich (USA), were used without further purification. Multilayer nanofilms of all four combinations of designed peptide were fabricated on negatively charged solid supports by layer-by-layer assembly (LBL).[1] The magnitude of the surface charge density

10.1021/bm060397k CCC: $33.50
Published on Web 07/15/2006

following cleaning (see below) was not necessarily the same for silver-coated quartz crystal microbalance (QCM) resonators, quartz slides, and silicon dioxide wafers. The substrates for film assembly had an area of 0.16 ± 0.01 cm^2, ~10 × 25 mm^2, and ~10 × 25 mm^2, respectively. In the first peptide adsorption step, P1 or P2 molecules were deposited by immersion of the substrate in 2 mg/mL peptide solution for 15 min. Loosely bound polycations were removed by rinsing the substrate 3× with deionized water, and the film was dried with N_2 gas. Then N1 or N2 molecules were deposited on the initial layer, and loosely bound polyanions were removed as before. The resulting bilayer was dried with N_2 gas, completing the first adsorption cycle. All nanofilms were dried for characterization ex situ. Diffusion of either adsorbing species within a film was therefore minimal. A total of 16 or 20 layers (8 or 10 bilayers) of peptide were deposited.

Nanofilms were built on QCM resonators (9 MHz nominal frequency; Sanwa Tsusho Co., Ltd, Japan) for determination of mass increment. The resonators were cleaned by immersion in acetone for 30 min and ultrasonication for 1−2 min, followed by thorough rinsing with deionized water and drying with N_2 gas. Shift in resonant frequency (Agilent 53131A 225 MHz universal counter, USA) was converted to mass increment by the Sauerbrey equation.[13] The mass sensitivity constant was 1.83 × 10^8 Hz·cm^2·g^{-1}. Nanofilms were built on quartz slides for characterization by spectroscopy in the ultraviolet range. Slides were cut into pieces and cleaned sequentially by agitation in hot 1% sodium dodecyl sulfate for 30 min, immersion into 1% NaOH in 99.8% CH_3OH/H_2O (50/50, v/v) for 2−3 h, and agitation in a hot 1:3 (v/v) mixture of 98% H_2SO_4 and 27% H_2O_2 for 5 min ("piranha"). Slides were stored in piranha solution, and they were rinsed thoroughly with deionized H_2O and dried with N_2 gas immediately before peptide film assembly experiments. Nanofilms were built on Si wafers (N/Phos-⟨100⟩, resistivity 1−10 ohm·cm, thickness 375−425 μm, diameter 100 ± 0.5 mm; Silicone Technology Corp., USA) for evaluation of thickness by ellipsometry (Sentech Instruments GmbH SE 850 ellipsometer, Germany). The wafers had a very thin layer of naturally grown SiO_2 on the Si surface. Wafers were cut into pieces in a clean room, rinsed with deionized H_2O, dried with N_2 gas, and stored in sealed dust-free vials.

Results

QCM analysis revealed that growth of a multilayer film of polycation P1 with polyanion N1 ("P1/N1") was "linear" from the macroscopic perspective under the conditions of the experiments (Figure 2a). A similar result was obtained for P2/N2. Linearity of growth was corroborated in both cases by optical spectroscopy (Figure S1, Supporting Information). More material was deposited in a given number of adsorption cycles for P2/N2, however, than for P1/N1. There are more charged groups in P1 or N1 than in P2 or N2, but a 1:1 peptide complex has a net charge of 0 in P1/N1 and in P2/N2. P2 is substantially more hydrophobic and less soluble in aqueous solution than P1.

Macroscopic growth of P1/N2 and of P2/N1, by contrast, was supralinear (Figure 2a). The inset of Figure 2a shows that buildup of the latter was exponential.[6,9] In these peptide systems, a 1:1 complex has a theoretical net charge of ±15 electronic charges; $|\lambda|$ is "mismatched", i.e., not the same for both assembly partners.

Salt concentration was a constant in the nanofilm assembly experiments reported here. This suggests that the observed difference in growth mode between P1/N1 and P2/N2 on one hand and P1/N2 and P2/N1 on the other hand might be attributable to the extent of "matching" of $|\lambda|$ or to a difference in hydrophobicity between the assembling polymers.

Polypeptides are weak polyelectrolytes; $|\lambda|$ can depend significantly on pH. P1 and N1 are highly charged at neutral pH. Figure 2a shows that little polymer was deposited in successive adsorption steps during P1/N1 assembly, consistent with earlier work on low molecular weight poly(L-lysine) (PLL) and poly(L-glutamic acid) (PLGA).[14] Strong electrostatic attractions and repulsions dominate polymer interactions in this system, particularly when the film is dry and the effective dielectric constant between molecules is reduced, promoting self-limited polymer adsorption and, as shown below, yielding an ultrathin and dense multilayer film. Similar behavior is shown by strong polyelectrolytes.[1]

$|\lambda|$ is "matched" in P2/N2, as in P1/N1, but P2 or N2 has a lower value of $|\lambda|$ than P1 or N1, and P2 or N2 is more hydrophobic than P1 or N1. Self-limited deposition is therefore

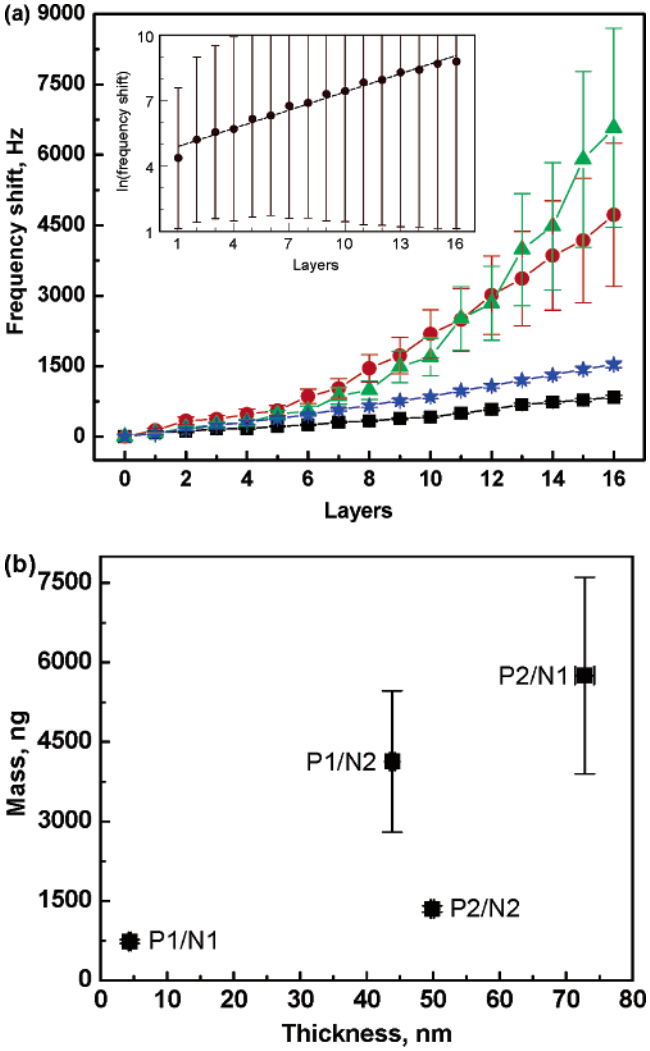

Figure 2. Peptide multilayer nanofilm assembly and thickness. (a) Analysis of nanofilm assembly by QCM. ■, P1/N1; ●, P1/N2; ▲, P2/N1; ★ P2/N2. P1/N1 and P2/N2 show linear growth; P1/N2 and P2/N1, supralinear growth. Variance in overall frequency shift increased with increasing adsorption step. Error bars represent the standard deviation of measurements made in four independent nanofilm assembly experiments. Inset, logarithm of frequency shift and uncertainty for P2/N1. The linear least-squares fit to all available data points (broken line) has a correlation coefficient $r > 0.99$. For 16 observations, the probability of exceeding this value of r in a random sample of observations taken from an uncorrelated parent population $p < 0.05\%$. (b) Density of peptide films. QCM film mass after 16 layers is plotted against ellipsometric film thickness after 20 layers. A substantial dependence of density on the combination of polymers is evident. For instance, the density and thickness of films containing N1 depends markedly on assembly partner. Uncertainties in thickness represent standard deviation of measurements made at three different points on the same sample.

less probable for P2 and N2 than for P1 and N1; hydrophobic interactions will compete less well than strong electrostatic interactions with thermal fluctuations. The degree of polymerization of the polymers and the ionic strength of solution were low in the experiments reported here, limiting the formation of "loops" and "tails" in adsorbed polymers,[8] minimizing increases in film surface roughness in successive layers and promoting organized self-assembly of peptides into a multilayer film.[15]

In P1/N2 and P2/N1, there is a difference in $|\lambda|$ between the assembling polymers. The presumed condition of charge neutrality within a polyelectrolyte multilayer film (e.g., ref 16) might require the relatively large mass deposition of the lower $|\lambda|$ peptides, for example, N2 molecules in the P1/N2 system, particularly at a low concentration of small counterions.

Ellipsometric film thickness was 4.4 ± 0.2 nm for P1/N1, 44 ± 0.4 nm for P1/N2, 73 ± 1.5 nm for P2/N1, and 50 ± 0.2 nm for P2/N2 (Figure 2b). Film refractive index was a fitting parameter; the best-fit values fell in the range 1.35−1.55 and varied inversely with film thickness. P1/N1, built of high $|\lambda|$ peptides, was the thinnest film by an order of magnitude. P2/N2 was somewhat thicker than P1/N2. The thickest film, however, P1/N2, was not the one built of the most hydrophobic peptides. These findings suggest that the complex interplay of electrostatic interactions, hydrophobic interactions, thermal fluctuations, and peptide solubility together will determine polymer assembly behavior and film growth mode.

Analysis of peptide multilayer nanofilms by atomic force microscopy confirmed that all films completely covered the substrate after deposition of 10 bilayers, and it revealed that film surface roughness was a function of film architecture (e.g., Figure S2, Supporting Information). Deswelling will have occurred on drying the film with N_2 gas, but the degree was almost certainly less than 70%, the amount obtained with 30−70 kDa PLL and 50−100 kDa PLGA at an ionic strength of ~0.15.[17] It is likely that the thickness of the designed peptide multilayer nanofilms on rewetting was similar to that before drying, as in the cited PLL/PLGA study.[17]

The density of dry P1/N1 was severalfold greater than that of dry P2/N2 (Figure 2b), despite the linearity of film assembly in both cases (Figure 2a). Presumably this difference reflects the relative contributions of electrostatic interactions and hydrophobic interactions to polymer adsorption; $|\lambda|$ is high in P1 and N1, it is half as much in P2 and N2, and P2 and N2 are rather hydrophobic. P1/N2 and P2/N1 show supralinear growth. These nanofilms are comparatively thick and dense. The differences in density between similar peptide systems suggest a limitation on the accuracy of estimates of film thickness based on mass measurement, a dubious but nevertheless common practice.

Average ellipsometric thickness per layer after 10 bilayers was 0.22 nm for P1/N1, 2.2 nm for P1/N2, 3.6 nm for P2/N1, and 2.5 nm for P2/N2. Given that the "thickness" of a polypeptide is about 1.2 nm (Figure 1) and that peptides studied here are likely to adopt a relatively extended conformation, because $|\lambda|$ is relatively large and the degree of polymerization is relatively small, the ellipsometry data suggest that multiple molecular layers are deposited per adsorption step in P1/N2, P2/N1, and P2/N2 but not in P1/N1.

Further examination of the data in Figure 2a suggests that they corroborate the hypothesis that multiple molecular layers are deposited per adsorption step. Let the frequency shift of polycation deposition for a given bilayer be Δf_+, and let that of the polyanion be Δf_-. The frequency shift ratio R for a given bilayer can be defined as $\Delta f_+/\Delta f_-$. When overall film growth is linear, R will depend on the relative amount of material deposited in successive adsorption steps. For example, if 3 times as much polycation is deposited as polyanion in a given adsorption cycle, then $R = 3$. R could be a function of extent of film growth, providing clues as to a possible change in mechanism for polyelectrolyte deposition near to and far from the influence of the substrate. R can be computed in cases of nonlinear film growth as an indicator of "microscopic" film growth behavior. As shown in Figure 3a, R tends to 1 for P1/N1 as the number of adsorption steps increases, hovers around 1 for P2/N2 and around 2 for P2/N1, and tends to 1/2 for P1/N2. The data suggest, for example, that twice as much P2 than N1 is deposited per adsorption step in P2/N1. Comparison of the molecular structures of the peptides suggests that differences in $|\lambda|$ or in hydrophobic surface area underlie this behavior. In P2/N2, where both peptides have $|\lambda| \approx 0.5$, both are hydrophobic, and both have the same distribution of charge, the mass increment will be independent of the number of layers deposited per adsorption step, if film surface roughness and charge density are approximately constant. Assuming two layers per adsorption step in P2/N2 and one in P1/N1, R will be 1.78 for adsorption of P2 in P2/N2 relative to adsorption of P1 in

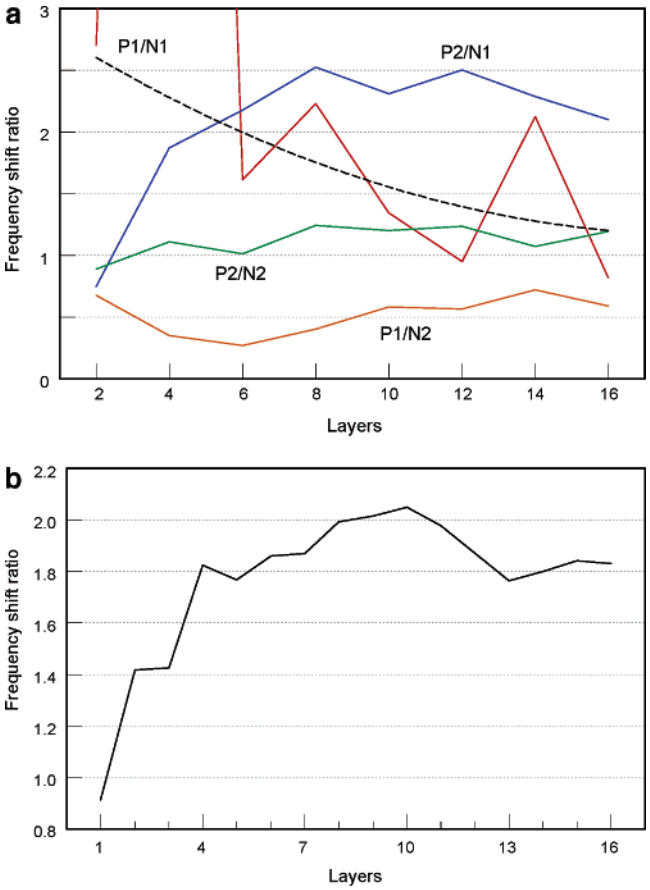

Figure 3. Frequency shift ratio R as a function of film buildup. (a) Frequency shift ratio for different combinations of peptides is plotted as a function of number of layers. As the number of layers deposited increases, P1/N1 tends to $R = 1$, P2/N2 hovers around 1, P2/N1 tends to 2 and P1/N2 hovers around 0.5. Scatter in the P1/N1 data are from the relatively large error in the QCM frequency shift measurements. P1/N1 layers are thin; little material is deposited per adsorption step. The broken line highlights the tendency of the P1/N1 data. See Figure S3 in the Supporting Information for uncertainty in R values. (b) Ratio of frequency shift R of P2/N2 to that of P1/N1 as a function of layer number (adsorption step). The calculation validates Model 2 for P2/N2 in Figure 4, which predicts a frequency shift ratio of 1.78 for P2 and P1 and a ratio of 1.79 for N2 and N1.

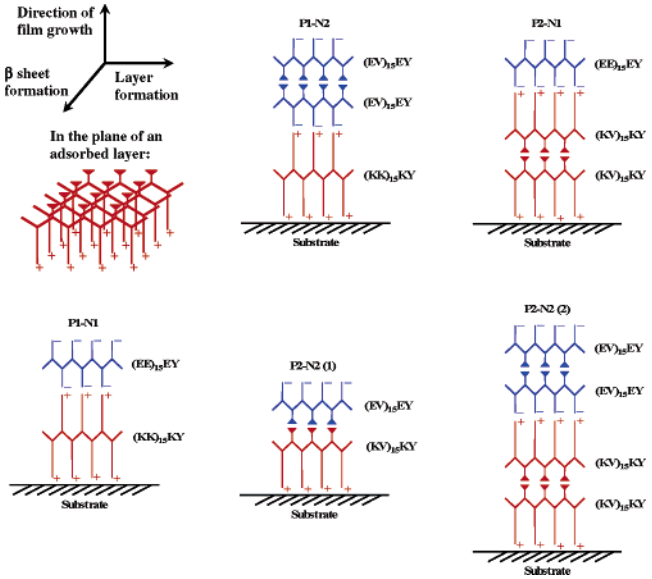

Figure 4. Structural models. There is but one adsorption mode for P1/N1, P1/N2, and P2/N1 but two for P2/N2. Model 1 of P2/N2, however, is substantially less plausible than model 2, as it would require exposure of a hydrophobic surface to a hydrophilic environment each $(KV)_{15}KY$ deposition step. More important, the experimental data reported in Figure 2 are more consistent with model 2 than model 1. The ratio of positive layers to negative layers in each case is 1:1, 1:2, 2:1, and 1:1, respectively. Multilayer formation with P2 and N2 resembles film formation from phospholipids.[29]

P1/N1, and 1.79 for N2 relative to N1, based on calculated peptide mass. Figure 3b shows the computed values of R for the data in Figure 2. The experimental data clearly tend to the predicted value.

Simple, first-approximation models of microscopic growth for all four peptide nanofilms are shown in Figure 4. The models are based in part on CD data, which show that a substantial proportion of peptide bonds in a polypeptide multilayer nanofilm are in β sheet conformation (Figure S1), but they take no account at all of surface roughness, polymer backbone flexibility, heterogeneity of molecule conformation due to thermal fluctuations, or film viscoelasticity; just $|\lambda|$ and hydrophobicity. Nevertheless, the measured values of R are remarkably consistent with model predictions, as shown in Figure 3. Deviation of the measured values from predictions could be due to changes in surface roughness during film growth. In any case, the QCM data, which show a relatively constant frequency shift from adsorption step to adsorption step, are more supportive of model 2 than model 1 for P2/N2. This stands to reason, as formation of a single layer of P2 or N2 on a charged substrate is improbable during deposition from an aqueous environment, given the hydrophobic nature of the valine side chain. The thickness increment is more than 10-fold larger for P2/N2 than P1/N1, not 2-fold larger, despite the frequency shift being just twice as great for P2/N2 as for P1/N1. The apparent discrepancy between QCM and ellipsometry could be due to the formation of aggregates of P2 or of N2 in solution (Figure S4) or to the thickness-related differences in optical properties of the nanofilms. In any case, P2/N2 is substantially less dense than P1/N1 (Figure 2b).

Discussion

Previous studies have shown that the poly(styrene sulfonate)/poly(allylamine hydrochloride) system, for example, shows linear growth and that the PLGA/PLL system shows supralinear growth at neutral pH and moderate ionic strength.[12] A change in mode for a given system from linear to supralinear growth can result from an increase in ionic strength of the polyelectrolyte deposition solutions.[5,17−20] The character of film buildup can also be influenced by details of the film fabrication process. For example, a pH or an ionic strength jump during or after film assembly can reduce surface roughness by an annealing process[21] and possibly result in pore formation.[22] Film structure can also be altered by drying.[23] Proposed mechanisms of growth mode under various conditions have been a source of controversy in the scientific literature. Polyelectrolyte self-assembly in multilayer nanofilm fabrication is akin to self-organization in protein folding when the polyelectrolytes are peptides.[24,25]

The data presented here show that the degree of "matching" of molecular properties between polypeptides influences film growth mode. For example, growth is linear in P1/N1, where $|\lambda|$ is matched, but growth is exponential in P2/N1, where $|\lambda|$ is not matched. For comparison, $|\lambda|$ is not matched in the PLL/hyaluronic acid (HA) system at pH 6.0−6.5,[12] as every other residue is ionizable in HA, and $|\lambda|$ is only approximately matched in the chitosan (CHI)/HA system at pH 5.0.[24] Nevertheless, both systems show what the respective authors call exponential film growth. In the cited studies, however, ionic strength was moderately high (0.15 M NaCl), increasing screening of polymer charges and decreasing persistence length, and films were not dried for characterization. PLL/HA is a particularly complex system because the unit lengths of the polymers are different, the degrees of freedom in the polymer backbone and in the side chains are different, the monomer masses differ by severalfold, the degrees of polymerization were different, the average polymer molecular weights were different, and the degrees of polydispersity were different. In the present work, by contrast, assembly data are shown for polyelectrolytes of the same unit length and approximately the same average number of degrees of freedom per monomer, monomer mass, degree of polymerization, and overall polymer mass. We decided to study the behavior of designed polypeptides to simplify the interpretation of growth mode data.

"Exponential" polyelectrolyte multilayer film growth is sometimes described as arising from polymer diffusion in a wet film. In the PLL/HA system, for example, the diffusing species is PLL.[6] $|\lambda| \approx 1$ for PLL under the conditions of the experiments (near neutral pH). In the present work, by contrast, experimental conditions were such that polymer diffusion was improbable or limited: The films were dried between adsorption steps and before measurement. Let us assume, however, that the exponential growth of P2/N1 resulted from polyion diffusion. Were P2 molecules or N1 molecules the species that diffused throughout the film? Let us suppose P2. Why then does P2/N2 show linear growth, as it too is built from P2? Do P2 molecules diffuse in the presence of N1 but not N2 molecules? If so, what is the physical basis of the difference in behavior in the two cases? Is it the difference in $|\lambda|$ between N1 and N2? Is it the difference in hydrophobic surface area? The difference in $|\lambda|$ or hydrophobic surface area must be responsible. Why should a smaller value of $|\lambda|$ for P2 than for N1 promote diffusion of P2 in the film? The diffusing species in the PLL/HA system is the more highly charged PLL.[6] So let us suppose that N1 molecules were the diffusing species in the P2/N1 system. Why then does P2/N1 show exponential growth but P1/N1 linear growth? The same form of logic applies to analysis of the P1/N2 system. The observed assembly behavior of P2/N1 and the conditions of these experiments together imply, then, that

exponential film growth might not have an essential dependence on the inward diffusion of polyelectrolytes.

Fibril formation of P2 or of N2 in solution[25,26] might increase the odds of exponential film growth in P2/N1 and P1/N2 by way of successive increases in surface roughness with increases in the number of layers deposited.[2,3,5] Growth of P2/N2, however, is linear, not exponential. Such behavior might be attributable to the similar solubility of the two peptides. That is, adsorbing N2 molecules might displace some adsorbed P2 molecules during adsorption, because the binding affinity to a surface of given absolute charge density is about the same for both polymers, and solubility is about the same for both polymers (both have the same number of charges per unit length and the same number of valine residues). In any case, the data are consistent with the view that "macroscopic" nanofilm growth arises not from peptide structure per se, but from the interaction of one type of polymer with its assembly partner. For example, growth of P1/N1 is linear but that of P2/N1 is exponential. Aggregation of P2 or N2 in solution (see Figure S4 in the Supporting Information) does not invalidate the models shown in Figure 4, because, idealized as they are, the simple models accurately predict the quantal nature of self-assembly of peptide layers evident in Figure 3. To some degree, then, the models must provide insight on the nature of the polypeptide film formation process.

Conclusions

Four 32mer peptides were designed for investigation of the physical basis of weak polyelectrolyte multilayer nanofilm assembly. All experiments were done at neutral pH and low ionic strength, and all films were dried prior to measurement. The results have revealed striking differences in the growth characteristics of the various combinations of peptide. Analysis suggests that "microscopic" properties of nanofilm growth will depend largely on the linear structures of the polymers and that "macroscopic" properties of film growth will depend on interactions between polymers. The self-assembly of peptides in a multilayer nanofilm resembles the self-organization of peptides in protein folding.[24,25] The results of this work provide more support for dry macroscopic polyelectrolyte multilayer film growth being governed primarily by surface area than by volume, even in cases of exponential increase in film mass per adsorption step. Polypeptide nanofilms are promising for the development of multifunctional materials and coatings for medical devices.[27] Elucidation of the underlying mechanisms of polypeptide multilayer nanofilm growth will inform related research on "fuzzy nanoassemblies", bionanomaterials, and protein folding.

Acknowledgment. We thank Dr Wang Yongmei and anonymous reviewers for helpful comments. This work was supported in part by a Nanoscale Exploratory Research award from the National Science Foundation (DMI-0403882), a seed grant from the Center for Entrepreneurship and Information Technology, a project grant from Artificial Cell Technologies, Inc., and the 2002 Capital Outlay Act 23 of the State of Louisiana (Governor's Biotechnology Initiative). The research of J.M.S. was supported by an NSF Research Experience for Undergraduate award (EEC-0244075).

Supporting Information Available. Details of optical thickness and surface morphology experiments, polypeptide nanofilm assembly data obtained by ultraviolet spectroscopy and circular dichroism spectrometry, surface morphology data obtained by atomic force microscopy, and uncertainty in frequency shift ratios. This material is available free of charge via the Internet at http://pubs.acs.org.

References and Notes

(1) Decher, G. *Science* **1997**, *277*, 1232−1237.
(2) Tsukruk, V. V.; Bliznyuk, V. N.; Visser, D.; Campbell, A. L.; Bunning, T. J.; Adams, W. W. *Macromolecules* **1997**, *30*, 6615−6625.
(3) Elbert, D. L.; Herbert, C. B.; Hubbell, J. A. *Langmuir* **1999**, *15*, 5355−5362.
(4) Lvov, Y. In *Protein Architecture: Interfacial Molecular Assembly and Immobilization Biotechnology*; Lvov, Y., Möhwald, H., Eds.; Marcel Dekker: New York, 2000; pp 125−167.
(5) Ruths, J.; Essler, F.; Decher, G.; Riegler, H. *Langmuir* **2000**, *16*, 8871−8878.
(6) Picart, C.; Mutterer, J.; Richert, L.; Luo, Y.; Prestwich; G. D.; Schaaf, P.; Voegel, J.-C.; Lavalle, P. *Proc. Natl Acad. Sci. U.S.A.* **2002**, *99*, 12531−12535.
(7) Decher, G., Schlenoff, J. B., Eds.; *Multilayer Thin Films: Sequential Assembly of Nanocomposite Materials*; Wiley-VCH: Weinheim, 2003.
(8) Hoogeveen, N. G.; Cohen Stuart, M. A.; Fleer, G. J.; Böhmer, M. R. *Langmuir* **1996**, *12*, 3675−3681.
(9) Haynie, D. T.; Zhang, L.; Zhao, W. *Polym. Mater. Sci. Eng.* **2005**, *93*, 94−97.
(10) E, glutamic acid; K, lysine; V, valine; Y, tyrosine. Tyrosine is for spectroscopic detection and quantitation.
(11) Creighton, T. E. *Proteins: Structures and Molecular Properties*, 2nd ed.; Freeman: New York, 1993.
(12) Picart, C.; Lavalle, P.; Hubert, P.; Cuisinier, F. J. G.; Decher, G.; Schaaf, P.; Voegel, J.-C. *Langmuir* **2001**, *17*, 7414−7424.
(13) Sauerbrey, G. *Z. Phys.* **1959**, *155*, 206−222.
(14) Haynie, D. T.; Balkundi, S.; Palath, N.; Chakravarthula, K.; Dave, K. *Langmuir* **2004**, *20*, 4540−4547.
(15) Zhang, L.; Li, B.; Zhi, Z.-l.; Haynie, D. T. *Langmuir* **2005**, *21*, 5438−5445.
(16) Schlenoff, J. B.; Ly, H.; Li, M. *J. Am. Chem. Soc.* **1998**, *120*, 7626−7634.
(17) Halthur, T. J.; Claesson, P. M.; Elofsson, U. M. *J. Am. Chem. Soc.* **2004**, *126*, 17009−17015.
(18) Kim, D. K.; Han, S. W.; Kim, C. H.; Hong, J. D.; Kim, K. *Thin Solid Films* **1999**, *350*, 153−160.
(19) McAloney, R. A.; Sinyor, M.; Dudnik, V.; Goh, C. M. *Langmuir* **2001**, *17*, 6656−6663.
(20) Sukhorukov, G. B.; Schmitt, J.; Decher, G. *Ber. Bunsen-Ges. Phys. Chem.* **1996**, *100*, 948−953.
(21) Mendelsohn, J. D.; Barrett, C. J.; Chan, V. V.; Pal, A. J.; Mayes, A. M.; Rubner, M. F. *Langmuir* **2000**, *16*, 5017−5023.
(22) Fery, A.; Scholer, B.; Cassagneau, T.; Caruso, F. *Langmuir* **2001**, *17*, 3779−3783.
(23) Lvov, Y.; Ariga, K.; Onda, M.; Ichinose, I.; Kunitake, T. *Colloids Surf., A* **1999**, *146*, 337−346.
(24) Haynie, D. T.; Zhang, L., Rudra, J. S.; Zhao, W.; Zhong, Y.; Palath, N. *Biomacromolecules* **2005**, *6*, 2895−2913.
(25) Li, B.; Rozas, J.; Haynie, D. T. *Biotechnol. Prog.* **2006**, *22*, 111−117.
(26) Richert, L.; Lavalle, P.; Payan, E.; Shu, X.-Z.; Prestwich, G. D.; Stoltz, J.-F.; Schaaf, P.; Voegel, J.-C.; Picart, C. *Langmuir* **2004**, *20*, 448−458.
(27) Brack, A.; Orgel, L. E. *Nature* **1975**, *256*, 383−387.
(28) Lamm, M. S.; Rajagopal, K.; Schneider, J. P.; Pochan, D. J. *J. Am. Chem. Soc.* **2005**, *127*, 16692−16700.
(29) Ariga, K. In *Handbook of Polyelectrolytes and Their Applications, Vol. 1 Polyelectrolyte-based Multilayers, Self-assemblies and Nanostructures*; Tripathy, S. K., Kumar, J., Nalwa, H. S., Eds.; American Scientific: Stevenson Ranch, CA, 2002; pp 99−126.

BM060397K